Simulation Based Study of On-chip Antennas for a Reconfigurable Hybrid 3D Wireless NoC

Ankit More and Baris Taskin

Department of Electrical and Computer Engineering, Drexel University
Philadelphia, Pennsylvania, USA 19104
E-mail: am434@drexel.edu, taskin@coe.drexel.edu

***Abstract*—The feasibility of using on-chip antennas for a reconfigurable 3D wireless network-on-chip (3D-WiNoC) on a 3D integrated circuit (IC) is shown. The reconfigurable 3D-WiNoC is designed with on-chip antennas which are proposed to be used in conjunction with the metal interconnects making it a hybrid design. The feasibility of the on-chip antennas is shown by performing a 3-D finite element method (FEM) based full wave electro-magnetic analysis on a 3D IC model. The 3D IC is modeled according to a complimentary metal oxide semiconductor (CMOS) silicon on insulator (SoI) Benzocyclobutene (BCB) polymer adhesive bonding 3-D circuit integration technology. It is shown that it is possible to have two different frequency domains for the signal sources and the dynamic switching of the signal sinks between the two frequency domains, with minimal design and area overhead. When implemented, the proposed hybrid network architecture with two frequency channels can reduce the latency and increase the network throughput.**

I. Introduction

The demand for high speed and high performance circuits has increased the trend of integrating large number of functional and storage cores onto a single die or system-on-chip (SoC). However, technology scaling of the devices provides new design challenges to the interconnect network that are required for communication between these functional and storage cores. Need for a global communication network between multiple cores on a SoC also increases the interconnect challenge. Technology scaling of the devices has increased the speed of the individual cores but it has also been accompanied by an increase in parasitics associated with the interconnects. The increased parasitics have caused the delay due to these interconnects to become higher than the gate delay [1]. The global interconnect networks therefore suffer from skew, jitter, power dissipation and area consumption [2], which has an increasing impact on the overall performance of the SoC [3].

The conventional design approaches introduced to mitigate the effect of the interconnect delay, such as changes to materials of the chip (e.g. use of low κ dielectrics and high conductivity metals), can increase the scaling of the global interconnect system only by a few technology generations [1]. Hence, there is a need for alternate design solutions at the interconnect or the architecture level. Contemporary design solutions, such as the networks-on-chip (NoC), have been proposed to structure the design of the on-chip inter-core communication infrastructure [4]. In addition, 3D integrated circuits (3D ICs) can alleviate the problems of skew, jitter and delay caused by scaling of metal interconnects in planar integrated circuits (ICs). 3D ICs also provide opportunities for integration of wafers manufactured using different manufacturing processes and a true system-on-a-chip (SoC) [5]. The performance improvements in using a 3D network-on-chip (3D-NoC), over traditional NoCs is shown in [6, 7].

The 3D ICs use through silicon vias (TSVs) for communication between the tiers of the 3D IC stack. However, the TSVs suffer from a considerable utilization of the wiring footprint of the individual tiers of the 3D IC leaving less area for intra-tier routing and device placement, thereby imposing constraints on the number of TSVs per unit area [5]. Moreover, the process of fabricating TSVs for a multi-tier (more than 2 tiers) interconnection on a 3D IC is difficult for some TSV technologies and entirely prohibited for certain others [5]. Further, if two (2) laterally separated communication end-points on two (2) separate tiers are to be connected, then intra-tier routing is necessary.

The proposed alternative to address the communication challenge is to use radio frequency (RF) interconnects. In the RF interconnect based NoCs, the data is transmitted from one communication end-point to the other using electromagnetic (EM) waves. As the EM waves travel at the speed of light in the medium, a low latency and high bandwidth communication can be achieved [8]. There are two (2) types of RF IC interconnects of note: The micro-strip transmission line based interconnects operating in the RF range [9] and the wireless communication based intra-chip interconnects operating in the RF range [10]. This paper focuses on the simulation based analysis of the latter to investigate adaptability to a NoC implementation.

The proposed NoCs with wireless interconnects do not antiquate wire-based interconnects or the TSVs; the wireless RF interconnects are proposed to be used selectively for critical paths. To this end, a hybrid 3D wireless NoC is proposed that integrates the wireless RF interconnects with traditional metal wire based interconnects. The network throughput and latency improvements using the hybrid wireless NoC (WiNoC) are shown in [4, 8, 11]. In this paper, the concept of the hybrid wireless NoCs is novelly extended to 3D-NoCs making it a 3D wireless network-on-chip (3D-WiNoC). As another major contribution, two different frequency channels are provided with

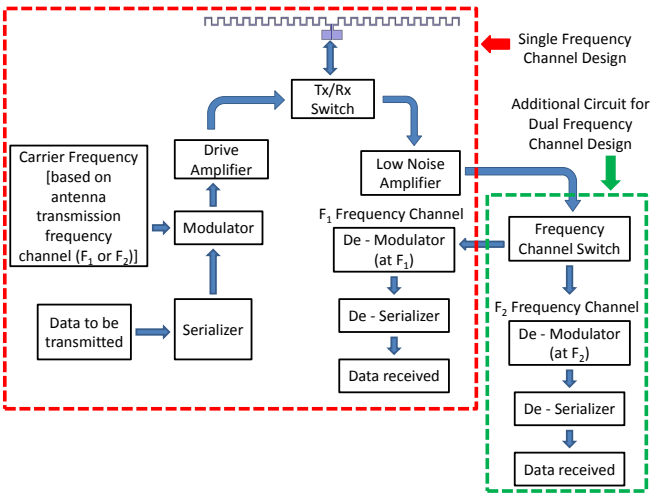

Fig. 1. Transceiver block diagram for the reconfigurable WiNoC.

inter channel communication capabilities, making the proposed 3D-WiNoC *reconfigurable*. Reconfigurability through multiple communication channels provides more flexibility to the network design and improves its latency with minimized area overhead.

This work is not a network analysis study but a feasibility study for the implementation and characterization of the proposed wireless RF interconnects. To this end, EM simulations are performed on the on-chip antennas on a 3D IC model. A network analysis study can only be performed after the feasibility and characterization of the antennas are well established. The proposed hybrid network architecture is presented in Section II. The simulation setup and the simulation results are discussed in Section III and Section IV, respectively. The key aspects of this paper are summarized in Section V.

II. Proposed Hybrid Network Architecture

The WiNoCs proposed in [8] have a transceiver optimized to operate at the transmission frequency of the antenna—making it a single frequency design—as illustrated in Figure 1. Under such a design, if there are multiple antennas transmitting data simultaneously, there is a high possibility of corruption of data due to the collision of the two signals [11]. In order to avoid collisions, a medium access control (MAC) protocol, such as the one described in [11], can be used (similar to time division multiplexing). However, using a MAC protocol adds to the latency in the system and decreases the network throughput. In this regard, if there are multiple frequency channels, the network throughput and latency can be improved by having different antennas transmitting data simultaneously on different frequency channels (frequency division multiplexing of the channel). Having multiple antennas for different frequency channels to communicate between two identical communication end-points would require multiple transceivers, each optimized for a single frequency. Such a design will increase the area overhead tremendously making it impractical for most systems.

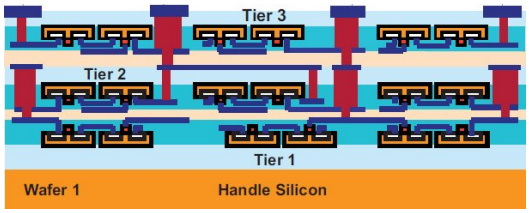

Fig. 2. 3D IC 3-tier integration structure.

In the proposed reconfigurable 3D-WiNoC design, the transceiver is designed with a receiver side operating at two receiving frequencies (F_1 and F_2) and with a transmitter side operating at a single frequency (F_1 or F_2) as illustrated in Figure 1. This design provides two different frequency channels for signal propagation with minimal increase in the circuit area overhead. The signal sources in this *reconfigurable* network design are grouped into one of the two frequency domains (F_1 or F_2). The reconfigurability in the network is due to the flexibility of the signal sinks (e.g. antennas) which can be moved dynamically into one of the two frequency domains (F_1 or F_2) with the frequency channel switch in Figure 1. Such a design is possible due to the characteristics of the antennas in the semiconductor implementation medium, as will be discussed in Section III and Section IV.

III. Wireless Interconnect Analysis

The feasibility of on-chip antennas for intra-chip communication on planar ICs is shown in [10, 12]. High-speed operation capabilities of deep sub-micron devices have enabled circuits to operate at frequencies above 10 GHz. Since the physical dimension of an antenna is inversely proportional to its operating frequency, it is possible to have small antennas fabricated on chip using standard CMOS foundry processes. In [13–15], full wave simulation based studies are performed to study new antenna designs, the antenna characteristics in the semiconductor medium and to investigate the medium of propagation of the EM waves. However, all the previous works analyze the antenna characteristics and performance on planar ICs. In this paper, the concept of using on-chip antennas for global wireless communication is extended to 3D ICs. It is critical, for this purpose, for the simulation model to correctly incorporate the environment of operation.

In this paper, the wireless interconnects using on-chip antennas for the proposed reconfigurable 3D-WiNoC are simulated on a three tier 3D IC stack. In particular, the on-chip antennas for wireless inter-tier communication are simulated for a polymer adhesive IC tier bonding, embodied in a silicon on insulator (SoI) process [16]. The on-chip antennas can potentially be used for any of the 3D IC wafer bonding techniques. The cross-section view of the SoI 3D IC 3-tier integration is illustrated in Figure 2.

The simulations are performed in Ansoft HFSS (High Frequency Structure Simulator), a 3D finite element method (FEM) based full-wave electro-magnetic simulator [17]. Meander dipole antennas are used in the simulation

TABLE I
MATERIAL CHARACTERISTICS OF DIFFERENT SILICON REGIONS ON A DIE.

Material	Conductivity (S/m)	Relative Permittivity
Silicon Dioxide	0	3.7
2000 Ω-cm Silicon Substrate	0.05	11.9
P-type Epitaxial Silicon	3636.36	11.9
N-type Epitaxial Silicon	1818.18	11.9

TABLE II
DIMENSIONAL PARAMETERS OF THE MEANDER DIPOLE ANTENNA.

Design Parameter	Magnitude
Arm Length (excluding bend lengths)	1.2 mm
Arm Run Length (including bend lengths)	2.4 mm
Bend Element Width	10 μm
Bend Element Length	60 μm
Antenna Thickness	630 nm

model as these antennas are more compatible with conventional CMOS technologies in having 90° bend angles. The antennas are designed with a total arm length (including the length of the meander segments) of 2.4 mm according to the parameters presented in [18]. Note that the parameters presented in [18] do not include a high conductivity epitaxial layer under the antennas. The presence of a high conductivity epitaxial layer can reduce the radiation frequency. Hence, to accurately model the environment of operation for the on-chip antennas, the conductivity parameters for the different materials on the die are used. These parameters are listed in Table I. The conductivity values are calculated from typical foundry parameters and doped semiconductor material resistivity data provided in [19]. The conductivity values do not change substantially from one technology generation to the other and therefore the design can easily be scaled with technology. The dimensional parameters for the meander dipole antennas are provided in Table II. The die size is 6×3.4 mm^2 as shown in Figure 3(a). The die size is selected arbitrarily to enable the integration of six (6) antennas of the dimensions reported in Table II. Varying the size of the dies impacts the presented simulations minimally.

The 3D-WiNoC is simulated for a six (6) antenna system. Two antennas are placed on each of the three IC tiers of the 3D IC stack with arbitrarily chosen lateral displacements of 5, 4, and 3 mm as shown in Figure 3(b) (antennas are depicted as black boxes). The antennas are identical, however placed near different epitaxial layers due to the semiconductor implementation medium. The difference in the transmitting frequency for these antennas with similar antenna structures is achieved due to the presence of high conductivity epitaxial layers under or above the antenna structures. The antennas placed on IC tiers 1 and 2 of the 3 tier IC stack are affected by two epitaxial layers with approximately equal separation for both set of antennas (antennas on tier 1 and tier 2). While the antennas placed on IC tier 3 are affected by two epitaxial layers placed closer than that for the antennas on IC tier 1 and 2 due to the 3D IC integration topology (face-to-face for IC tier 2 and face-to-back for IC tier 3 [5]).

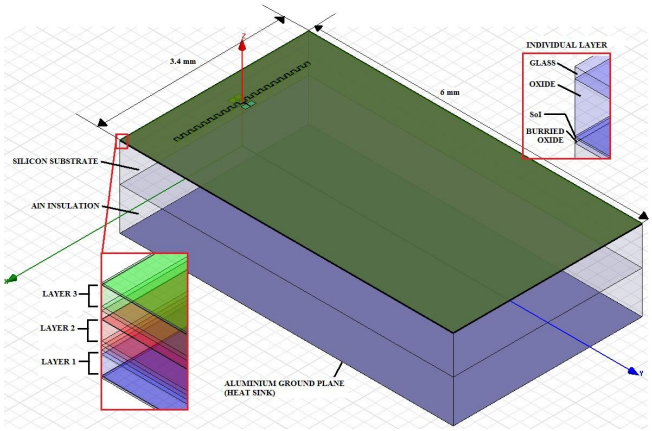

(a) Simulated 3D IC structure.

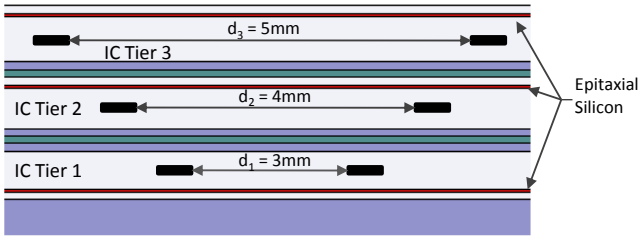

(b) Antenna placement.

Fig. 3. Simulation setup for the reconfigurable WiNoC on a SoI 3DIC.

Hence, the transmitting frequency of the antennas on IC tiers 1 and 2 is similar while that of the antennas on IC tier 3 is different, thereby providing two different frequency channels for communication. The frequency range for the simulation is selected to be between 9 GHz to 15 GHz, based on the frequency range achievable with the antenna sizes.

IV. RESULTS AND DISCUSSIONS

In experimentation, the scattering parameter (s-parameter) matrix $\overline{S}$ for the network is collected. The s-parameter matrix of a network characterizes the coupling between the ports of a network. An element, S_{ij} of the s-parameter matrix $\overline{S}$ is the ratio of the normalized output power at port i due to the normalized input power at port j [20]. The s-parameter S_{ii}, also defined as the return loss, is used to determine the radiation frequency of the transmitting antenna. The s-parameter S_{ij} characterizes the signal coupling between the receiving antenna i and the transmitting antenna j. Hence, the s-parameter matrix is used to characterize the operation and efficiency of the reconfigurable 3D-WiNoC system.

As discussed in Section III, the presence of a thin high-conductivity epitaxial layer near the antenna structure shifts the radiation frequency. This characteristic of the 3D IC medium in having different epitaxial layers in different tiers creates two different frequency channels for communication using a single antenna design. The return loss (based on the maximum absolute value) of the antennas on different tiers is shown in Figure 4.

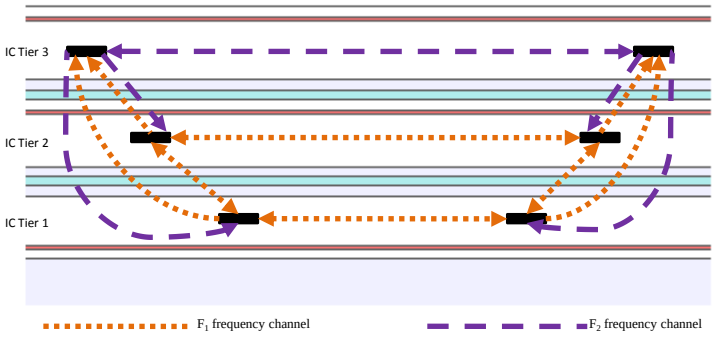

Fig. 5. The reconfigurable 3D-WiNoC with F_1 and F_2 frequency channels.

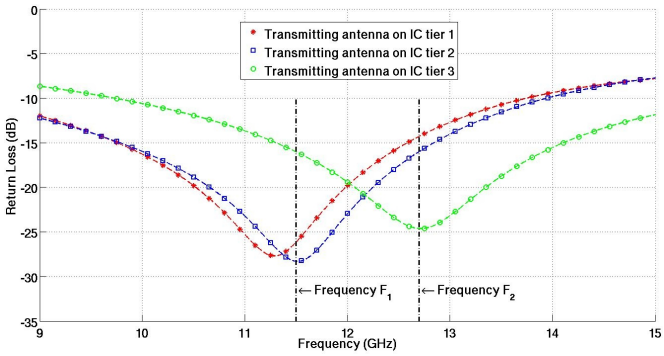

Fig. 4. Return loss S_{11} at the transmitting antenna.

The lowest point of the dip indicates the frequency where the return loss is minimum; this is the frequency at which the antennas radiate energy most efficiently and therefore describes the frequency of operation of the antenna. As expected, the antennas on IC tier 1 and 2 operate at similar frequencies of $F_1 \approx 11.5\ GHz$ while the antennas on IC tier 3 operate at a different frequency of $F_2 \approx 12.7\ GHz$. These two frequencies provide the two different frequency channels for communication as depicted in Figure 5.

The figure of merit for an antenna pair is the transmission gain G_a between the transmitting and receiving antenna. The transmission gain, G_a of the antenna pair is computed using the following formula:

$$G_a = \frac{|S_{ij}|^2}{(1-|S_{ii}|^2)(1-|S_{jj}|^2)} = G_t G_r \left(\frac{\lambda}{4\pi R}\right)^2 e^{-2\alpha R} \quad (1)$$

where S_{ij} is the forward transmission between the receiving antenna i and the transmitting antenna j, S_{ii} is the reflection of the electric field at the receiving antenna and S_{jj} is the reflection of the electric field at the transmitting antenna. G_t and G_r are the gains of the transmitting and receiving antennas, respectively, λ is the wavelength of the electromagnetic waves based on the effective dielectric constant ϵ_r, α is the attenuation constant and R is the separation between the transmitting and receiving antennas.

All the parameters S_{ii}, S_{jj}, and S_{ij} are embodied in the s-parameter matrix $\overline{S}$ obtained from the 3D FEM analysis. A high value of the transmission gain indicates a good signal coupling. For an effective communication, it is required that the gain of the antenna pair be higher than the gain that can be provided using a low noise amplifier (LNA) at the receiving end. CMOS integrated LNAs are capable of providing gains as high as 50 dB [21], hence any transmission gain above a threshold of -50 dB is considered a communication channel.

Based on the return loss presented in Figure 4, the antennas on IC tier 1 transmit in the F_1 frequency channel in the transmitting mode. The strength of the signal coupling and the wireless channel indicated by the transmission gain between a transmitting antenna on any IC tier and a receiving antenna on IC tier 1 is shown in Figure 6. The transmission gain between a transmitting antenna on IC tier 1 and a receiving antenna on IC tier 1 communicating in the frequency channel F_1 is shown in Figure 6(a). The transmission gain between a transmitting antenna on IC tier 2 and a receiving antenna on IC tier 1 communicating in the frequency channel F_1 is shown in Figure 6(b). The transmission gain between a transmitting antenna on IC tier 3 and a receiving antenna on IC tier 1 communicating in the frequency channel F_2 is shown in Figure 6(c). Thus, in the receiving mode the antennas can receive signals in both the frequency channels F_1 and F_2. The transceiver can be switched from the transmitting mode to the receiving mode, or vice-versa, through the *Tx/Rx switch* shown in Figure 1. The receiver side of the transceiver can also be switched from frequency F_1 to F_2, or vice-versa, through the *frequency channel switch* as depicted in Figure 1. Similarly, the strength of the signal coupling and the wireless channel to a receiving antenna on IC tier 2 or IC tier 3 is shown in Figure 7 and Figure 8, respectively.

The transmission gain in all the cases is higher than the -50 dB threshold indicating an achievable effective communication between the transmitting and receiving antennas. The transmission distances achievable are higher than the ones assumed in [4, 8, 11], thereby providing a larger range for a single hop communication. The larger range of operation decreases the latency and increases the network throughput. The transmission gain will be lower for a larger lateral separation of antennas and higher for a smaller lateral separation of antennas as it is inversely proportional to the separation between the antennas as explained by (1).

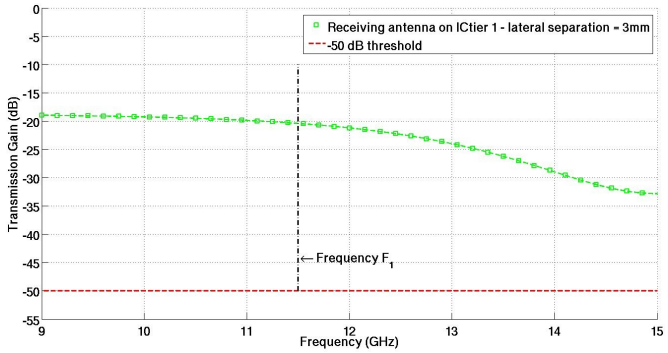

(a) Received signal from antenna on IC tier 1 at frequency F_1.

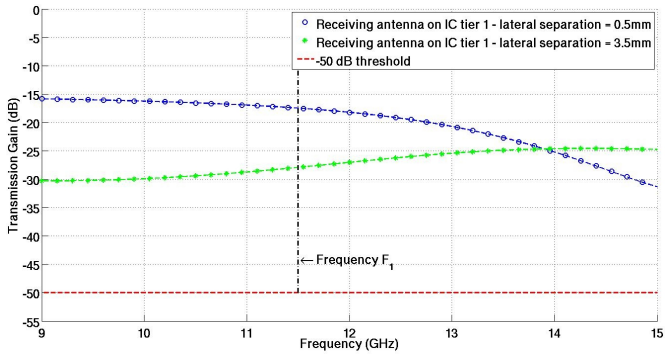

(b) Received signal from antennas on IC tier 2 at frequency F_1.

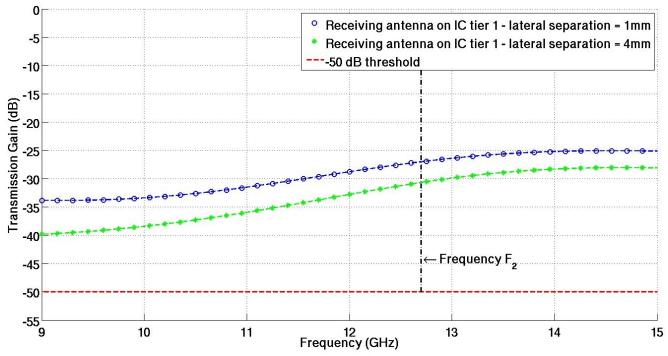

(c) Received signal from antennas on IC tier 3 at frequency F_2.

Fig. 6. Transmission gains for receiving antennas on IC tier 1.

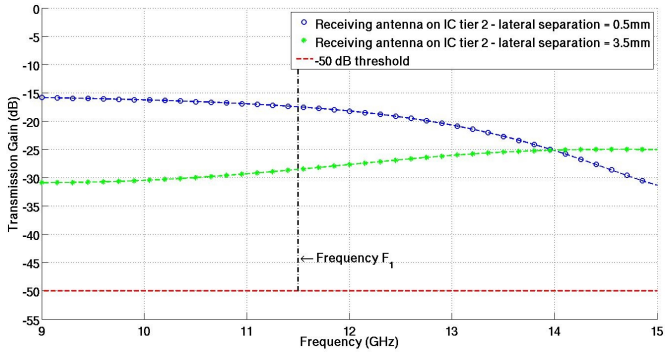

(a) Received signal from antennas on IC tier 1 at frequency F_1.

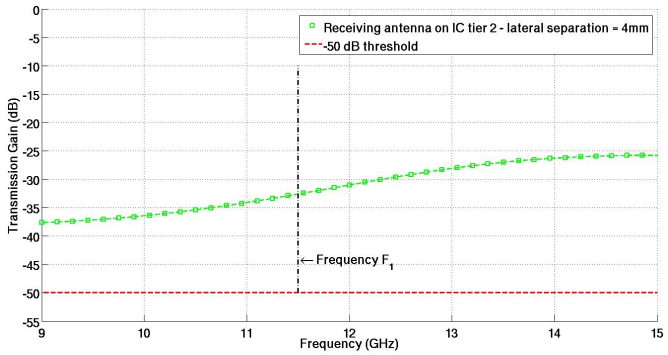

(b) Received signal from antenna on IC tier 2 at frequency F_1.

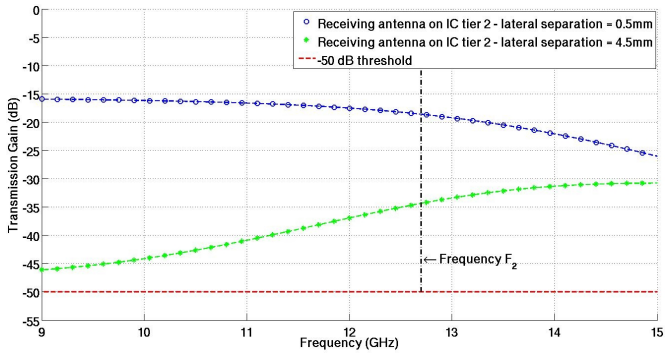

(c) Received signal from antennas on IC tier 3 at frequency F_2.

Fig. 7. Transmission gains for receiving antennas on IC tier 2.

The dynamic switching of the receiver between the two frequency domains provides the reconfigurability of the network. The reconfigurability is implementable due to the characteristics of the antennas in the semiconductor medium. The transmission gain between the antennas transmitting at frequency $F_1 \approx 11.5\ GHz$ (antennas on IC tier 1 and 2) and the receiving antennas (antennas on IC tier 3) (which transmit at frequency $F_2 \approx 12.7\ GHz$) is above the -50 dB threshold at frequency F_1, as shown in Figure 8(a) and Figure 8(b), thereby providing good signal coupling. Similarly, for the antennas transmitting at frequency F_2 (antennas on IC tier 3), the transmission gain between the F_1 and F_2 frequency channel antennas is above the -50 dB threshold at frequency F_2, as shown in Figure 6(c) and Figure 7(c), respectively.

V. Summary of Results

Based on the discussion in Section IV it is concluded that:

1) It is possible to have simultaneous communication between different communication end-points in two different frequency channels ($F_1 \approx 11.5\ GHz$ and $F_2 \approx 12.7\ GHz$ in the simulated environment).
2) The network has the following properties:
   a) The antennas in the transmitting mode on IC tier 1 and IC tier 2 are signal sources for the F_1 frequency channel and the antennas in the transmitting mode on IC tier 3 are the signal sources for the F_2 frequency channel.
   b) The signal sinks (antennas in the receiving mode on IC tier 1, IC tier 2 and IC tier 3) can be switched dynamically between either of the two

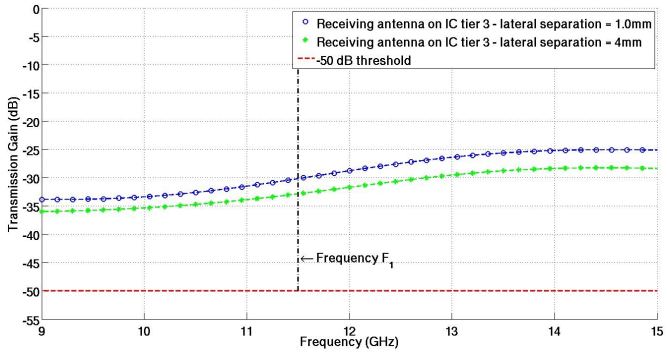

(a) Received signal from antennas on IC tier 1 at frequency F_1.

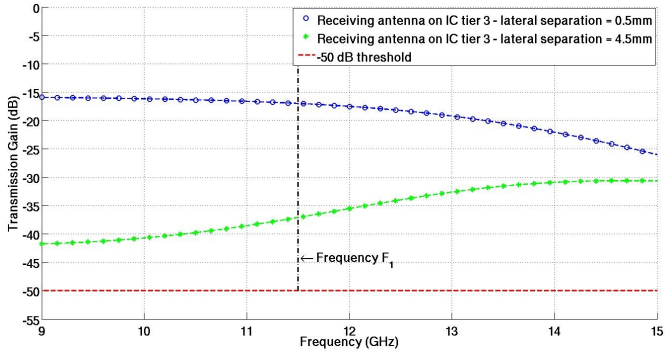

(b) Received signal from antennas on IC tier 2 at frequency F_1.

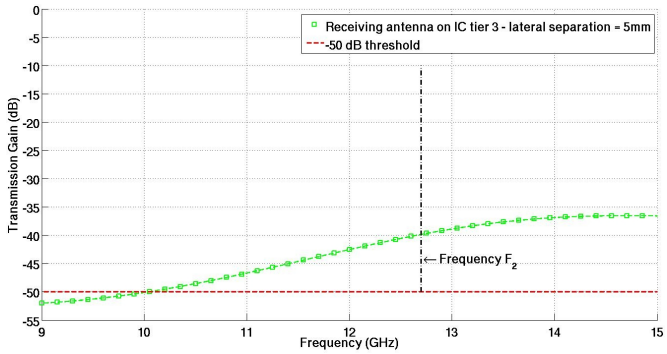

(c) Received signal from antenna on IC tier 3 at frequency F_2.

Fig. 8. Transmission gains for receiving antennas on IC tier 3.

frequency domains (F_1 or F_2) by switching the frequency channel switch depicted in Figure 1 to the appropriate channel using a control signal.

VI. Conclusion

In this work, the feasibility of using on-chip antennas for a reconfigurable hybrid 3D wireless network-on-chip (reconfigurable 3D-WiNoC) is shown. Since the antennas and the associated circuitry are expected to occupy a considerable amount of space, they are intended to be used in conjunction (i.e. hybrid operation) with metal interconnects based 3D-NoC. This work discusses the feasibility and characterization of on-chip antennas for reconfigurable 3D-WiNoCs from a signal coupling point of view.

It is shown that it is possible not only to have a strong communication channel but also to have communication in two frequency channels. The two channels and the reconfigurable operation of the same antenna between the channels can provide improvements in the network latency and the throughput. The reconfigurability of the signal sinks in the network is achieved with a minimal area overhead.

References

[1] *ITRS International Technology Roadmap for Semiconductors*, 2006.

[2] V. Mehrotra and D. Boning, "Technology scaling impact of variation on clock skew and interconnect to silicon," in *Proceedings of the IEEE International Interconnect Technology Conference (IITC)*, June 2001, pp. 122–124.

[3] R. Ho, K. W. Mai, and M. A. Horowitz, "The future of wires," in *Proceedings of the IEEE*, April 2001, pp. 490–504.

[4] L. P. Carloni, P. Pande, and Y. Xie, "Networks-on-chip in emerging interconnect paradigms: Advantages and challenges," in *Proceedings of the ACM/IEEE International Symposium on Networks-on-Chip (NOCS)*, May 2009, pp. 93–102.

[5] P. Garrou, C. Bower, and P. Ramm, *Handbook of 3D Integration: Technology and Applications of 3D Integrated Circuits*. Wiley, 2008.

[6] B. Feero and P. P. Pande, "Network-on-chip in a three dimensional environment: A performance evaluation," *IEEE Transactions on Computers*, vol. 58, pp. 32–45, January 2009.

[7] D. Park, S. Eachempati, R. Das, A. K. Mishra, Y. Xie, N. Vijaykrishnan, and C. R. Das, "Mira: A multi-layered on-chip interconnect router architecture," in *In Proceedings of the IEEE International Symposium on Computer Architecture (ISCA)*, June 2008, pp. 251–261.

[8] P. P. Pande, A. Ganguly, K. Chang, and C. Teuscher, "Hybrid wireless network on chip: A new paradigm in multi-core design," in *Proceedings of the International Workshop on Network on Chip Architectures (NoCArc)*, December 2009, pp. 71–76.

[9] M. F. Chang, V. P. Roychowdhury, L. Zhang, H. Shin, and Y. Qian, "RF/wireless interconnect for inter- and intra-chip communications," *Proceedings of the IEEE*, vol. 89, pp. 456–466, April 2001.

[10] B. A. Floyd, C. M. Hung, and K. K. O, "Intra-chip wireless interconnect for clock distribution implemented with integrated antennas, receivers and transmitters," *IEEE Journal of Solid-State Circuits*, vol. 37, pp. 543–551, May 2002.

[11] D. Zhao, "Ultraperformance wireless interconnect nanonetworks for heterogeneous gigascale multi-processor socs," in *Proceedings of the Workshop on Chip Multiprocessor Memory Systems and Interconnects (CMP-MSI)*, June 2008.

[12] K. Kim, "Design and characterization of RF components for inter- and intra- chip wireless communication," Ph.D. dissertation, University of Florida, 2000.

[13] M. Bialkowski and A. Abbosh, "Investigations into intra chip wireless interconnection for ultra large scale integration technology," in *Proceedings of the IEEE Antennas and Propagation Society International Symposium (APSURSI)*, June, pp. 1–4.

[14] M. Sun, Y. P. Zhang, G. X. Zheng, and W. Y. Yin, "Performance of intra-chip wireless interconnect using on-chip antennas and UWB radios," *IEEE Transactions on Antennas and Propagation*, vol. 57, pp. 2756–2762, September 2009.

[15] A. More and B. Taskin, "Leakage current analysis for intra-chip wireless interconnects," in *Proceedings of the IEEE International Symposium on Quality Electronic Design (ISQED)*, March 2010, pp. 49–53.

[16] Y. Kwon, A. Jindal, R. Augur, J. Seok, T. S. Cale, R. J. Gutmann, and J. Q. Lu1, "Evaluation of BCB bonded and thinned wafer stacks for three-dimensional integration," *Journal of the Electrochemical Society*, vol. 155, pp. H280–H286, March 2008.

[17] *High Frequency Structure Simulator: User's Guide*, 10th ed., Ansoft Corporation, June 2005.

[18] H. Nakano, H. Tagami, A. Yoshizawa, and J. Yamauchi, "Sortening ratios of modified dipole antennas," *IEEE Transactions on Antennas and Propagation*, vol. 32, pp. 385–386, April 1984.

[19] J. M. Rabaey, A. Chandrakasan, and B. Nikolic, *Digital Integrated Circuits*, 2nd ed. Prentice Hall, 2003.

[20] D. M. Pozar, *Microwave Engineering*, 3rd ed. Wiley, 2005.

[21] A. B. M. H. Rashid, N. Sultana, M. R. Khan, and T. Kikkawa, "Efficient design of integrated antennas on Si for on-chip wireless interconnects in multi-layer metal process," *Japanese Journal of Applied Physics*, vol. 44, pp. 2756–2760, April 2005.